第 31 卷第 9 期
2015 年 9 月

无 机 化 学 学 报
CHINESE JOURNAL OF INORGANIC CHEMISTRY

Vol.31 No.9
1894-1902

羧酸桥联的四核镧系簇合物的磁热效应和慢磁弛豫

刘遂军[1,2] 崔 雨[1] 宋伟朝[1] 王庆伦[1] 卜显和*,[1]

([1]南开大学化学系,金属与分子基材料化学天津市重点实验室,天津化学化工协同创新中心,天津 300071)

([2]江西理工大学冶金与化学工程学院,赣州 341000)

摘要: 在水热条件下,通过使用羧酸和螯合配体得到了一个系列的四核镧系簇合物,即$[Ln_4(mnba)_{12}(tzp)_2(H_2O)_2]$(Ln=Gd (**1**), Tb (**2**), Er (**3**); Hmnba=间硝基苯甲酸; tzp=2-(1*H*-1,2,4-三唑-3-基)吡啶))。这 3 个化合物是同构的,且具有线性的四核簇结构。磁性研究表明,化合物 **1** 和 **3** 中簇内镧系离子之间是弱铁磁耦合的,但化合物 **2** 中铽离子之间是弱的反铁磁相互作用和(或)铽离子激发的斯塔克能级的去布居。化合物 **1** 具有较大的磁热效应($-\Delta S_m^{max}$=20.6 J·kg^{-1}·K^{-1})。交流磁化率测试表明化合物 **3** 展现出频率和温度依赖的虚部信号,这是慢磁弛豫的典型特征,原因是铒离子的强各向异性和铁磁耦合的存在。

关键词: 羧酸; 镧系簇合物; 磁热效应; 慢磁弛豫

中图分类号: O614.33+9; O614.341; O614.344 **文献标识码**: A **文章编号**: 1001-4861(2015)09-1894-09

DOI: 10.11862/CJIC.2015.240

Carboxylate-Bridged Tetranuclear Lanthanide Clusters: Magnetocaloric Effect and Slow Magnetic Relaxation

LIU Sui-Jun[1,2] CUI Yu[1] SONG Wei-Chao[1] WANG Qing-Lun[1] BU Xian-He*,[1]

([1]*Department of Chemistry, TKL of Metal- and Molecule-Based Material Chemistry and Collaborative Innovation Center of Chemical Science and Engineering* (*Tianjin*), *Nankai University, Tianjin* 300071, *China*)

([2]*School of Metallurgical and Chemical Engineering, Jiangxi University of Science and Technology, Ganzhou, Jiangxi* 341000, *China*)

Abstract: By using carboxylate and chelating ligands, a family of tetranuclear lanthanide clusters, namely $[Ln_4(mnba)_{12}(tzp)_2(H_2O)_2]$ (Ln=Gd (**1**), Tb (**2**) and Er (**3**), Hmnba=m-nitrobenzoic acid, tzp=2-(1*H*-1,2,4-triazol-3-yl) pyridine), has been obtained under hydrothermal conditions. The three complexes exhibit linear tetranuclear clusters bridged by carboxylates with *syn*, *syn*-μ_2-η^1:η^1 mode. Magnetic investigation indicates weak ferromagnetic interaction between adjacent Gd$^{\text{Ⅲ}}$ or Er$^{\text{Ⅲ}}$ ions of the Ln_4 cluster in **1** and **3**, while weak intra-molecular antiferromagnetic interaction between Tb$^{\text{Ⅲ}}$ ions and/or depopulation of the Tb$^{\text{Ⅲ}}$ excited Stark sub-levels in **2**. Complex **1** exhibits a significant magnetocaloric effect with $-\Delta S_m^{max}$=20.6 J·kg^{-1}·K^{-1} and ac susceptibility measurements reveal frequency- and temperature-dependent out-of-phase signal under 5 kOe dc field in **3**, being typical slow magnetic relaxation behavior due to strong anisotropy of Er$^{\text{Ⅲ}}$ and ferromagnetic coupling. CCDC: 978830, **1**; 978831, **2**; 978832, **3**.

Key words: carboxylate; lanthanide clusters; magnetocaloric effect; slow magnetic relaxation

收稿日期:2015-06-08。收修改稿日期:2015-07-22。

国家自然科学基金(No.21290171),江西省科技厅青年自然科学基金(No.20151BAB213003)资助项目。

*通讯联系人。E-mail:buxh@nankai.edu.cn

0 Introduction

The investigation of lanthanide (Ln) clusters has recently become an active field for their both fascinating structures and exceptional applications as molecular coolers and single-molecule magnets (SMMs)[1-6]. On one hand, $Gd^{Ⅲ}$ clusters could be regarded as candidate materials for magnetic refrigerators because of negligible magnetic anisotropy (D), large spin ground state (S) and low-lying excited spin states of $Gd^{Ⅲ}$ ion and weak couplings between $Gd^{Ⅲ}$ ions [7-11]. Generally, the entropy change ($-\Delta S_m$) is employed to represent the magnetocaloric effect (MCE) of molecular magnetorefrigerants[12-13]. The magnetic intensity (M_w/N_{Gd}) and magnetic interaction (θ) between $Gd^{Ⅲ}$ ions are proposed to be main factors to affect MCE for the Gd-type magnetic refrigerants [14-16]. To reduce M_w/N_{Gd} ratio and $|\theta|$ value of $Gd^{Ⅲ}$ complexes, the utilization of light ligands to synthesize $Gd^{Ⅲ}$ clusters supply an effective tool.

On the other hand, Ln-based SMMs with large energy barriers have been a hot research topic for molecular magnets compared with 3*d*/3*d*-4*f* based SMMs[17-19]. $Ln^{Ⅲ}$ clusters (especially for $Tb^{Ⅲ}$, $Dy^{Ⅲ}$, $Ho^{Ⅲ}$ and $Er^{Ⅲ}$ types) have recently become favorable candidates to explore SMMs, since the S and D of $Ln^{Ⅲ}$ ions could lead to an relatively large anisotropic energy barrier (U_{eff}) that prevents the reversal of the molecular magnetization[20-21].

Till now, most of Ln-clusters were constructed from Schiff-base and calix[4]arenes ligands with their chelating characteristic[22-25]. The mixed-ligand strategy, especially the utilization of carboxylates and N-donor ligands, has been employed to construct discrete clusters and coordination polymers as a powerful synthetic approach, while the design and synthesis of discrete Ln-clusters with unique structures and magnetic properties still remain a great challenge because of different affinities and coordination capabilities of the $Ln^{Ⅲ}$ ions to O-donors and N-donors[26-27].

As an extension of our studies on the synthesis and magnetic investigation of $Ln^{Ⅲ}$ complexes[28-31], herein, we choose sterically hindered Hmnba (m-nitrobenzoic acid) and corner ligands 2-(1*H*-1,2,4-triazol-3-yl) pyridine) (tzp) to construct low-dimensional structures (Scheme 1). Fortunately, a series of tetranuclear $Ln^{Ⅲ}$ clusters, namely $[Ln_4(mnba)_{12}(tzp)_2(H_2O)_2]$ (Ln=Gd (**1**), Tb (**2**) and Er (**3**)) were successfully synthesized.

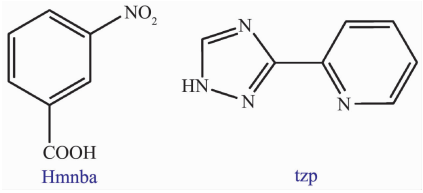

Scheme 1　Ligands used for the synthesis of **1**~**3**

Magnetic analyses reveal that complex **1** is weakly ferromagnetic coupled with $-\Delta S_m^{max}$=20.6 $J \cdot kg^{-1} \cdot K^{-1}$ for ΔH=7 T at 2.0 K and complex **3** displays slow relaxation of the magnetization. Strong quantum tunnelling effect excludes the existence of slow magnetic relaxation for **2** although 2 kOe dc field was exerted.

1 Experimental

1.1 Materials and instrumentation

All chemicals were of reagent grade and used as purchased without further purification. Elemental analysis (C, H and N) was performed on a Perkin-Elmer 240C analyzer (Perkin-Elmer, USA). The X-ray powder diffraction (PXRD) spectra were recorded on a Rigaku D/Max-2500 diffractometer at 60 kV, 300 mA for a Cu-target tube and a graphite monochromator. Simulation of the PXRD spectra were carried out by the single-crystal data and diffraction-crystal module of the Mercury (Hg) program available free of charge via the Internet at http://www.iucr.org. IR spectra were measured in the range of 400~4 000 cm^{-1} on a Tensor 27 OPUS FT-IR spectrometer using KBr pellets (Bruker, German). Magnetic data were measured by a Quantum Design MPMS-XL-7 SQUID magnetometer. Diamagnetic corrections were estimated by using Pascal constants and background corrections by experimental measurement on sample holders.

1.2 Preparation of 1~3

$[Gd_4(mnba)_{12}(tzp)_2(H_2O)_2]$ (**1**): A mixture of Gd_2O_3 (181 mg, 0.5 mmol), Hmnba (334 mg, 2 mmol) and tzp (66.6 mg, 0.5 mmol) in 10 mL H_2O was sealed in a Teflon-lined autoclave and heated to 160 ℃ for 2

days. After the autoclave was cooled to room temperature in 12 h, Cubic colorless crystals were collected with 30% yield based on $Gd^{Ⅲ}$. Anal. Calcd. for $C_{98}H_{64}O_{50}N_{20}Gd_4$ (%): C, 39.89; H, 2.19; N, 9.49. Found(%): C, 39.78; H, 2.78; N, 9.35. IR (KBr, cm^{-1}): 3 579m, 3 504m, 3 161m, 3 087s, 2 901m, 2 765w, 1 580 s, 1 483s, 1 344s, 1 263s, 1 166m, 1 080s, 995w, 912m, 831m, 788s, 725s, 651m, 576w, 523w, 416m.

$[Tb_4(mnba)_{12}(tzp)_2(H_2O)_2]$ (**2**): The same procedure as that for **1** was used for this complex except that Gd_2O_3 (181 mg, 0.5 mmol) was replaced by Tb_2O_3 (183 mg, 0.5 mmol) and the holding time is 3 days. Block colorless crystals were collected with ~40% yield based on $Tb^{Ⅲ}$. Anal. Calcd. for $C_{98}H_{64}O_{50}N_{20}Tb_4$(%): C, 39.80; H, 2.18; N, 9.47. Found(%): C, 40.13; H, 2.89; N, 9.60. IR (KBr, cm^{-1}): 3 494w, 3 157w, 3 080m, 2 893 m, 2 767w, 1 598s, 1 517s, 1 415s, 1 350s, 1 266m, 1 082 m, 995w, 910w, 790m, 723s, 649w.

$[Er_4(mnba)_{12}(tzp)_2(H_2O)_2]$ (**3**): The same procedure as that for **1** was used for this complex except that Gd_2O_3 (181 mg, 0.5 mmol) was replaced by Er_2O_3 (191 mg, 0.5 mmol) and the holding time is 3 days. Block pink crystals were collected with ~30% yield based on $Er^{Ⅲ}$. Anal. Calcd. for $C_{98}H_{64}O_{50}N_{20}Er_4$(%): C, 39.36; H, 2.16; N, 9.37. Found (%): C, 39.64; H, 2.78; N, 9.43. IR (KBr, cm^{-1}): 3 496w, 3 163w, 3 083m, 2 891w, 1 608s, 1 525s, 1 478s, 1 410s, 1 346s, 1 267m, 1 166w, 1 079m, 1 001w, 909w, 830w, 719s, 650m, 584w, 518w, 413w.

1.3 Crystallographic data and structure refinements

The single-crystal X-ray diffraction data of **1**~**3** were collected on a Rigaku SCX-mini diffractometer at 293(2) K with Mo $K\alpha$ radiation (λ=0.071 073 nm) by ω scan mode. The program CrystalClear[32] was used for the integration of the diffraction profiles. The structures were solved by direct method using the SHELXS program of the SHELXTL package and refined by full-matrix least-squares methods with SHELXL[33]. The non-hydrogen atoms were located in successive difference Fourier syntheses and refined with anisotropic thermal parameters on F^2. All hydrogen atoms of ligands were generated theoretically at the specific atoms and refined isotropically with fixed thermal factors. The hydrogen atoms of water in **1**~**3** were added by the difference Fourier maps and refined with suitable constrains. A summary of the crystallographic data, data collection, and refinement parameters for **1**~**3** is provided in Table 1.

CCDC: 978830, **1**; 978831, **2**; 978832, **3**.

Table 1 Crystal data and structure refinements for 1~3

	1	**2**	**3**
Formula	$C_{98}H_{64}O_{50}N_{20}Gd_4$	$C_{98}H_{64}O_{50}N_{20}Tb_4$	$C_{98}H_{64}O_{50}N_{20}Er_4$
Formula weight	2 950.69	2 957.37	2 990.73
Crystal system	Triclinic	Triclinic	Triclinic
Space group	$P\bar{1}$	$P\bar{1}$	$P\bar{1}$
a / nm	1.068 7(2)	1.063 5(2)	1.060 2(2)
b / nm	1.401 2(3)	1.392 3(3)	1.392 5(3)
c / nm	1.993 3(4)	1.977 3(4)	1.972 4(4)
α / (°)	70.33(3)	70.49(3)	71.06(3)
β / (°)	86.67(3)	86.71(3)	87.15(3)
γ / (°)	76.42(3)	76.40(3)	76.48(3)
V / nm^3	2.731 4(9)	2.681 5(9)	2.676 9(9)
D_c / ($g\cdot cm^{-3}$)	1.794	1.831	1.855
Z	1	1	1
F(000)	1 448	1 452	1 464
μ / mm^{-1}	2.504	2.714	3.212
Collected reflections	28 415	23 302	28 489

Continued Table 1

Unique reflections	12 390	9 453	12 231
R_{int}	0.036 5	0.042 3	0.046 7
R_1^a / wR_2^b [$I>2\sigma(I)$]	0.038 7 / 0.073 1	0.043 4 / 0.094 4	0.044 6 / 0.068 6
GOF on F^2	1.081	1.132	1.063

[a] $R=\sum(||F_o|-|F_c||)/\sum|F_o|$; [b] $wR=[\sum w(|F_o|^2-|F_c|^2)^2/(\sum w|F_o|^2)^2]^{1/2}$

2　Results and discussion

2.1　Synthesis

The mix-ligand strategy has been employed to construct the linear Ln-clusters successfully. As effective terminal co-ligands, tzp plays a key role in the formation of discrete lanthanide clusters. Compared with lanthanide salts, the use of Ln_2O_3 provides not only a slow-release $Ln^{Ⅲ}$ ion source but also a pH regulator of the reactions.

2.2　Description of crystal structures

Single crystal X-ray analysis reveals that **1**~**3** are isostructural, thus only the structure of **1** is described in detail. Complex **1** crystallizes in the triclinic space group $P\bar{1}$ with the asymmetric unit including two $Gd^{Ⅲ}$ ions, six mnba ligands, one tzp ligand and one coordinated H_2O. Gd1 is located in a seven coordinated environment constructed with seven O atoms from one water molecule and six carboxylates. Gd2 center exhibits an eight-coordinated environment with two N atoms of one tzp ligand and six carboxylate O atoms from five mnba ligands. Gd1 and Gd2 are connected by four carboxylate groups with *syn*, *syn*-μ_2-η^1:η^1 to form a linear Gd_4 cluster (Fig.1).

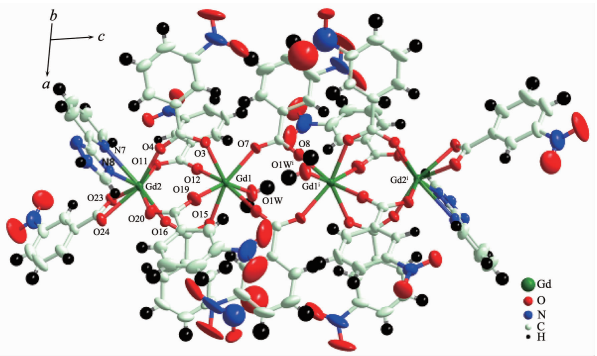

Symmetry code: [i] −*x*+1, −*y*+1, −*z*+2

Fig.1　View of the molecular structure showing 30% probability thermal ellipsoids of **1**

2.3　Magnetic studies

The magnetic properties of **1**~**3** were studied by solid state magnetic susceptibility measurements in 2.0~300 K range at 1 kOe dc field and the isothermal field-dependent magnetizations $M(H)$ at fields up to 70 kOe at 2.0 K. Before the magnetic measurements of **1**~**3**, their crushed crystalline samples were used to measure X-ray powder diffraction (PXRD, Fig.S1, SI) to confirm their phase purities.

Complex **1** contains isotropic $Gd^{Ⅲ}$(f^7) with a ground state $^8S_{7/2}$, and the first excited state $^6P_{7/2}$ is very high in energy, while complexes **2** and **3** include other anisotropic $Ln^{Ⅲ}$ ions. Generally, the magnetism of lanthanide (Ln) clusters is very difficult to explain because of the exchange-coupling and large orbital contributions as well as the crystal field perturbation[34-35]. The magnetic properties in the form of $\chi_M T$ vs T plots of **1**~**3** are shown in Fig.2. The room-temperature $\chi_M T$ products estimated as 31.45 (**1**), 46.39 (**2**) and 47.96 (**3**) emu·mol^{-1}·K are in relative good agreement with the presence of four lanthanide metal ions: four $Gd^{Ⅲ}$ ions (S =7/2, L=0, J=7/2, g=2, C=7.88 emu·mol^{-1}·K) for **1**, four $Tb^{Ⅲ}$ ions (S=3, L=3, J=6, g=3/2, C=11.82 emu·mol^{-1}·K) for **2** and four $Er^{Ⅲ}$ ions (S=3/2, L=6, J=

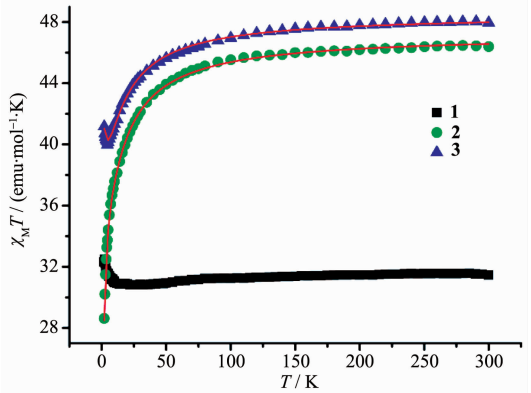

Red lines represent the best fitting

Fig.2　Plots of $\chi_M T$ vs T for **1**~**3**

15/2, g=6/5, C=11.48 emu·mol^{-1}·K) for **3**. For **1**, as the temperature decreases, the $\chi_M T$ value stays nearly constant in the high temperature range with a value of 30.86 emu·mol^{-1}·K at 14 K. Upon further cooling the temperature to 2.0 K, $\chi_M T$ abruptly increases to a maximum value (32.31 emu·mol^{-1}·K, indicating the ferromagnetic (F) interaction between Gd$^{\text{Ⅲ}}$ ions in the Gd_4 cluster. For **2**, up lowering of the temperature to 2.0 K, $\chi_M T$ value stays nearly constant at high temperatures, and then decreases sharply to a minimum value (28.62 emu·mol^{-1}·K), which indicates weak antiferromagnetic (AF) interaction in the Tb_4 cluster and/or depopulation of the Tb$^{\text{Ⅲ}}$ excited Stark sublevels. The Stark sub-levels of the anisotropic Tb$^{\text{Ⅲ}}$ ions may be progressively thermally depopulated leading to a decrease of the $\chi_M T$ value. For **3**, as the temperature decreases, the value of $\chi_M T$ slowly decreases down to a minimum value of 39.96 emu·mol^{-1}·K at 4.5 K. On cooling the temperature to 2 K, $\chi_M T$ abruptly increases to the maximum value (41.17 emu·mol^{-1}·K), indicating ferromagnetic coupling between Er$^{\text{Ⅲ}}$ ions in the Er_4 cluster.

The magnetizations slowly increase and tend to a value of 27.77$N\beta$ at 70 kOe, and the experimental magnetization plot of **1** is nearly consistent with the red line that presents the Brillouin function for four magnetically uncoupled Gd$^{\text{Ⅲ}}$ ions with S=7/2 and g=2.0, which further confirms the weak F behavior for **1** as similar literatures[3-4] (Fig.3a). The field dependences of the magnetizations at 2.0 K for **2** and **3** show rapid increases of the magnetizations at low fields, reaching about 16.13$N\beta$ and 19.87$N\beta$ at 10 kOe, and linear increases at high fields without achieving a complete saturation at 70 or 50 kOe (22.90$N\beta$ for **2** and 23.57 $N\beta$ for **3**, Fig.3b and 3c), which could be explained by the fact that the depopulation of the Stark levels of the Ln$^{\text{Ⅲ}}$ $^{2S+1}L_J$ ground state under the ligand-field perturbation produces a much smaller effective spin.

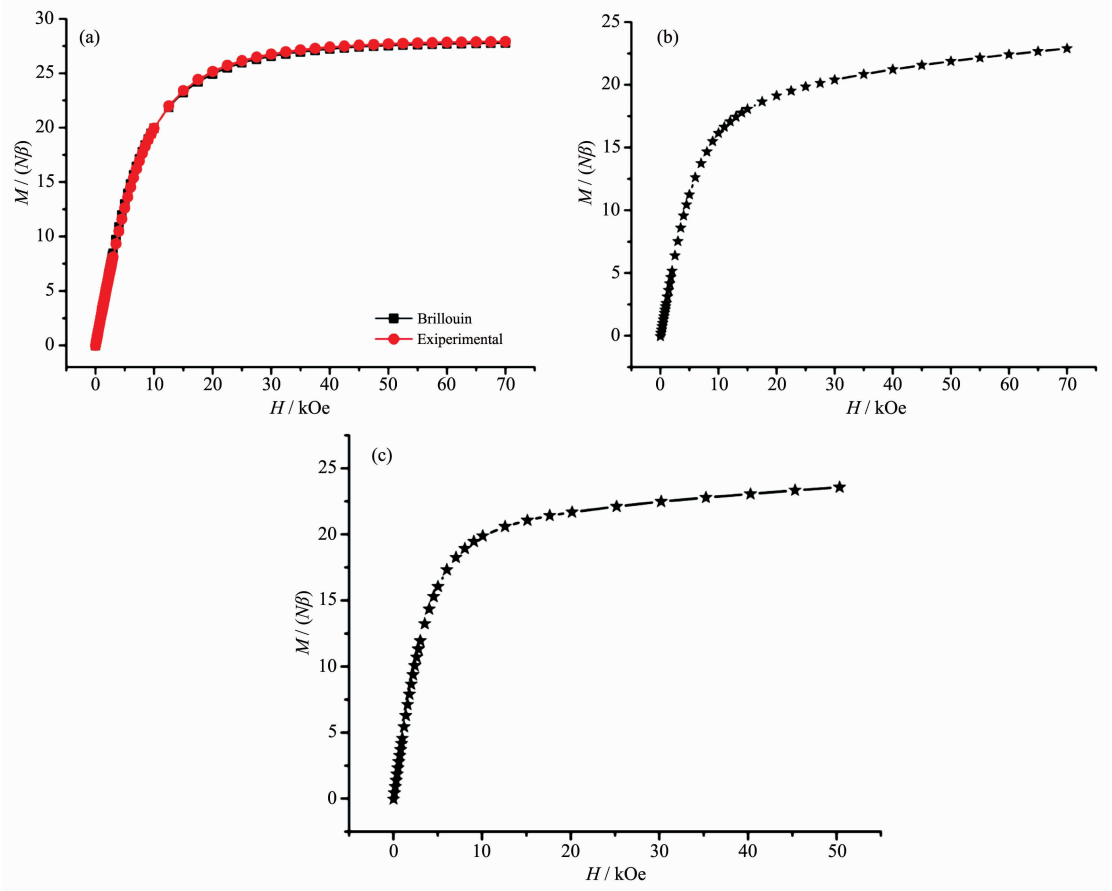

Red solid line represents Brillouin function of four magnetically isolated Gd$^{\text{Ⅲ}}$ ions with S=7/2 and g=2.0

Fig.3 M vs H curves of **1** (a), **2** (b) and **3** (c) at 2.0 K

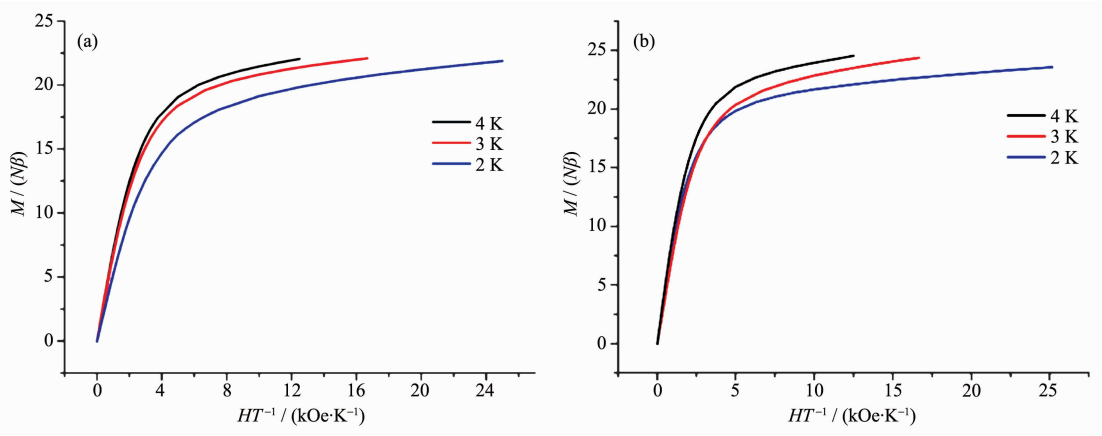

Fig.4　Curves of M vs H/T for **2** (a) and **3** (b)

For **2** and **3**, the M vs H/T (Fig.4) data at 2~4 K shows non-superposition plots and a rapid increase of the magnetization at low fields without any sign of saturation at 50 kOe. The reason is most likely because of anisotropy and important crystal-field effect at the Tb$^{\text{Ⅲ}}$ or Er$^{\text{Ⅲ}}$ ions, which eliminates the degeneracy of the $^7F_6$ and $^4I_{15/2}$ ground states. Reduced magnetization curves do not superimpose, further indicating the presence of a significant magnetic anisotropy and/or low lying excited states[15].

The recently developed non-critical scaling theory could be used to study the F/AF behaviors of **2** and **3** based on the sum of two exponential functions (as shown in Eq.**1**)[36-38].

$$\chi T=A\exp(E_1/T)+B\exp(E_2/T) \qquad (\mathbf{1})$$

In Eq.**1**, $A+B$ is the high-temperature extrapolated Curie constant and E_1 and E_2 denote the magnitude of the intracluster magnetic interaction. The first term in Eq.**1** represents an F/AF contribution to the moment that is dominant at low temperatures, whereas the second term reflects the crystal-field effect because the interionic interactions between the internal 4*f* electrons are usually very weak. The best fit of the experimental data gives that $A+B$=47.22 emu·mol^{-1}·K, E_1=−0.61 K and E_2=−20.94 K for **2** and $A+B$=48.54 emu·mol^{-1}·K, E_1=0.08 K and E_2=−18.12 K for **3** (Fig.2). The small values of E_1 of **2** and **3** further indicate very weak magnetic interactions between the Tb$^{\text{Ⅲ}}$/Er$^{\text{Ⅲ}}$ ions, which is in good agreement with the prediction that the Ln-Ln interaction is expected to be very weak, due to the shielding of the f-orbitals and the consequent poor overlap with the bridging ligand orbitals[12].

To characterize the low-temperature behaviors of **1**, the temperature dependencies of field-cooled (FC) and zero-field-cooled (ZFC) magnetization were measured under a field of 50 Oe upon warming from 2.0 K (Fig.5). The FC curve coincides with the ZFC curve and the magnetizations increase monotonically with the decrease of temperature, and no maximum is observed. These results indicate that **1** does not exhibit magnetic ordering above 2.0 K.

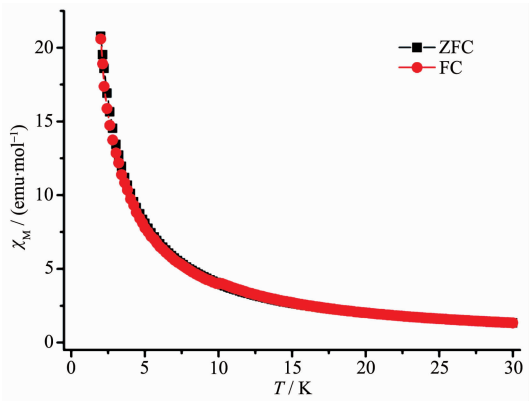

Fig.5　FC/ZFC curves at 2~30 K for **1**

Considering the weak magnetic couplings between the Gd$^{\text{Ⅲ}}$ ions and potential application of Gd$^{\text{Ⅲ}}$ complexes for magnetic refrigeration, we investigated the magnetocaloric properties of **1**. We used the magnetic entropy change (ΔS_m) to evaluate MCE, which could be calculated by the Maxwell equation $(\Delta S_m(T)_{\Delta H}=\int[\partial M(T,H)/\partial T]_H dH)$[39-41]. According to the equation, we could obtain the $-\Delta S_m$ from the experimental magnetization data

(Fig.6a), and the curves of $-\Delta S_m$ are depicted in Fig. 6b. The obtained $-\Delta S_m^{max}$ gives the value of 20.6 $J\cdot kg^{-1}\cdot K^{-1}$ (the theoretical $-\Delta S_m^{max}$ is 23.4 $J\cdot kg^{-1}\cdot K^{-1}$ calculated with $-\Delta S_m^{max}=4R\ln(2S+1)$, R is the gas constant) for a field change of 7 T at 2.0 K. If $-\Delta S_m^{max}$ is given per unit of volume, it is equivalent to 36.96 $mJ\cdot cm^{-3}\cdot K^{-1}$. Although various discrete $Gd^{Ⅲ}$ clusters have been constructed, their magnetocaloric properties have rarely been reported. Previous literatures report only twelve $Gd^{Ⅲ}$ clusters with significant MCE ($-\Delta S_m^{max}>20$ $J\cdot kg^{-1}\cdot K^{-1}$), as shown in Table 2.

To investigate possible SMM behaviors of **2** and **3**, alternating current (ac) susceptibility measurements were carried out in the temperature range of 15~2.0 K under H_{dc}=0 Oe and H_{ac}=3.5 Oe for variable frequencies (from 1 488 to 10 Hz). Unfortunately, although all the in-phase curves (χ') are almost consistent without peaks, there is no frequency dependent out-of-phase signal even up to 997 Hz (Fig.S2a and S2c). In order to weaken the quantum tunneling effect, 2 kOe dc field were applied to further study the dynamic properties. The ac signal of **2** is still poor and slow magnetic relaxation is not observed (Fig.S2b), while there is weak frequency dependent out-of-phase signal for **3**

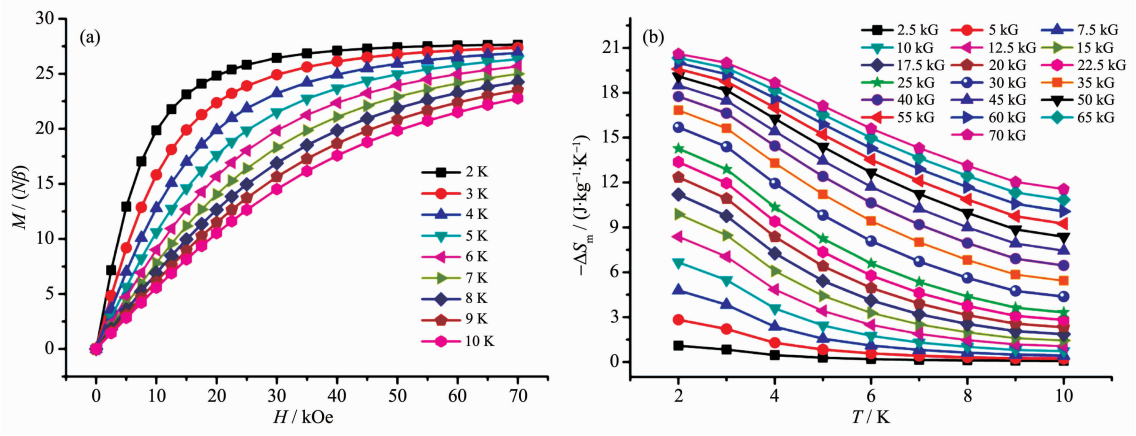

Fig.6 (a) M vs H curves of **1** at T=2~10 K and H=2.5~70 kOe; (b) Experimental $-\Delta S_m$ obtained from magnetization data of **1** at different fields and temperatures

Table 2 Comparison of $-\Delta S_m^{max}$ (larger than 20.0 $J\cdot kg^{-1}\cdot K^{-1}$) among 1 and $Gd^{Ⅲ}$ clusters associated with potential molecule-based magnetic coolers*

Complex	M_w / N_{Gd}	Magnetic interaction (θ / K)	$-\Delta S_m^{max}$ / ($J\cdot kg^{-1}\cdot K^{-1}$) ($\Delta H$)	$-\Delta S_m^{max}$ / ($mJ\cdot cm^{-3}\cdot K^{-1}$)
$[Gd_{104}]$[42]	292.44	AF (−4.11)	46.9 (7 T)	138.12
$[Gd_{24}]$[10]	340.40	AF (−0.16)	46.12 (7 T)	89.98
$[Gd_{48}]$[11]	313.83	AF (−3.57)	43.6 (7 T)	120.7
$\{[Gd(OAc)_3(H_2O)_2]_2\}\cdot 4H_2O$[13]	406.44	F (0.32)	41.6 (7 T)	82.78
$[Gd_{38}]$[11]	376.27	AF (−2.99)	37.9 (7 T)	102.0
$[Gd_4(OAc)_4(acac)_8(H_2O)_4]$[12]	432.53	F (0.23)	37.7 (7 T)	70.24
$[Gd_{10}]$[43]	463.59	AF	37.4 (7 T)	43.01
$[Gd_6]$[44]	434.65	F	33.5 (7 T)	56.68
$[Gd_3]$[44]	572	AF	31.3 (7 T)	64.99
$[Gd_{10}(3\text{-}TCA)_{22}(\mu_3\text{-}OH)_8(H_2O)_4]$[8]	457.76	AF (−1.78)	31.22 (7 T)	68.64
$[Gd_4]$[45]	632.19	AF	27.2 (7 T)	40.96
$[Gd_2(OAC)_2(Ph_2acac)_6(MeOH)_2]$[12]	694.81	F (0.18)	23.7 (7 T)	36.43
$[Gd_7]$[9]	549.09	AF	23 (7 T)	41.33
$[Gd_4(mnba)_{12}(tzp)_2(H_2O)_2]$ (**1**)	737.67	F (0.51)	20.6 (7 T)	36.96

*$-\Delta S_m^{max}$ / ($mJ\cdot cm^{-3}\cdot K^{-1}$)=[$-\Delta S_m^{max}$ / ($J\cdot kg^{-1}\cdot K^{-1}$)]·[$D_c$ / ($g\cdot cm^{-3}$)]

(Fig.S2d). Then 5 kOe dc field was exerted and attempted to obtain better ac signals. Therefore, the peaks can be observed obviously both in χ_M' and χ_M'' curves (see Fig.7), which suggested the existence of slow magnetic relaxation behavior in **3**. As aforementioned, strong anisotropy of $Er^{Ⅲ}$ ions and weak ferromagnetic interaction presumably lead to the field-induced slow magnetic relaxation behavior in **3**.

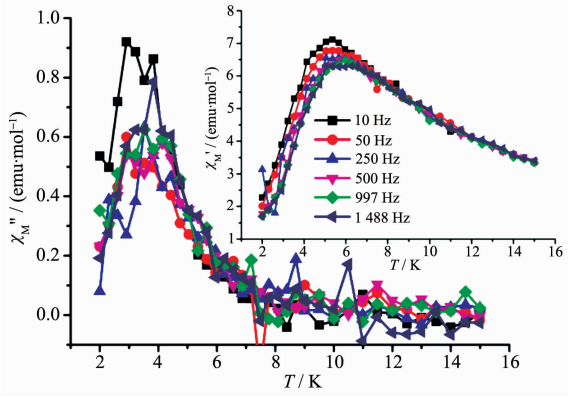

Fig.7　Temperature dependence of the ac χ_M at different frequencies for **3** with H_{dc}=5 kOe

3　Conclusions

A type of linear tetranuclear lanthanide clusters (**1**~**3**) constructed from the monocarboxylate and terminal co-ligand has been synthesized in hydrothermal reactions. Magnetic investigation indicates that **1**~**3** are weakly coupled with **1** displaying large MCE with $-\Delta S_m^{max}$=20.6 $J\cdot kg^{-1}\cdot K^{-1}$ and **3** exhibiting slow magnetic relaxation behavior for the strong anisotropy and ferromagnetic contribution. Complex **2** does not show slow magnetic relaxation behavior because of weak antiferromagnetic interaction and strong quantum tunneling effect, although 2 kOe dc field was exerted.

References:

[1] Zheng Y Z, Zhou G J, Zheng Z, et al. *Chem. Soc. Rev.*, **2014**, **43**:1462-1475

[2] Sharples J W, Collison D. *Polyhedron*, **2013**,**54**:91-103

[3] Woodruff D N, Winpenny R E P, Layfield R A. *Chem. Rev.*, **2013**,**113**:5110-5148

[4] Liu J L, Chen Y C, Guo, F S, et al. *Coord. Chem. Rev.*, **2014**,**281**:26-49

[5] Rinehart J D, Long J R. *Chem. Sci.*, **2011**,**2**:2078-2085

[6] Habib F, Murugesu M. *Chem. Soc. Rev.*, **2013**,**42**:3278-3288

[7] Wang P, Shannigrahi S, Yakovlev N L, et al. *Chem. Asian J.*, **2013**,**8**:2943-2946

[8] Liu S J, Zhao J P, Tao J, et al. *Inorg. Chem.*, **2013**,**52**:9163-9165

[9] Sharples J W, Zheng Y Z, Tuna F, et al. *Chem. Commun.*, **2011**,**47**:7650-7652

[10]Chang L X, Xiong G, Wang L, et al. *Chem. Commun.*, **2013**, **49**:1055-1057

[11]Guo F S, Chen Y C, Mao L L, et al. *Chem. Eur. J.*, **2013**, **19**:14876-14885

[12]Guo F S, Leng J D, Liu J L, et al. *Inorg. Chem.*, **2012**,**51**: 405-413

[13]Evangelisti M, Roubeau O, Palacios E, et al. *Angew. Chem. Int. Ed.*, **2011**,**50**:6606-6609

[14]Liu S J, Xie C C, Jia J M, et al. *Chem. Asian J.*, **2014**,**9**: 1116-1122

[15]Lorusso G, Sharples J W, Palacios E, et al. *Adv. Mater.*, **2013**,**25**:4653-4656

[16]Han S D, Miao X H, Liu S J, et al. *Inorg. Chem. Front.*, **2014**,**1**:549-552

[17]Blagg R J, Muryn C A, McInnes E J L, et al. *Angew. Chem. Int. Ed.*, **2011**,**50**:6530-6533

[18]Gao F, Cui L, Liu W, et al. *Inorg. Chem.*, **2013**,**52**:11164-11172

[19]Guo Y N, Xu G F, Wernsdorfer W, et al. *J. Am. Chem. Soc.*, **2011**,**133**:11948-11951

[20]Jiang S D, Liu S S, Zhou L N, et al. *Inorg. Chem.*, **2012**,**51**: 3079-3087

[21]Jiang S D, Wang B W, Sun H L, et al. *J. Am. Chem. Soc.*, **2011**,**133**:4730-4733

[22]Rell N M, Anwar M U, Drover M W, et al. *Inorg. Chem.*, **2013**,**52**:6731-6742

[23]Anwar M U, Thompson L K, Dawe L N, et al. *Chem. Commun.*, **2012**,**48**:4576-4578

[24]Liu C M, Zhang D Q, Hao X, et al. *Cryst. Growth Des.*, **2012**,**12**:2948-2954

[25]Xu X, Zhao L, Xu G F, et al. *Dalton. Trans.*, **2011**,**40**:6440-6444

[26]Liu S J, Zhao J P, Song W C, et al. *Inorg. Chem.*, **2013**,**52**: 2103-2109

[27]Sessoli R, Powell A K. *Coord. Chem. Rev.*, **2009**,**253**:2328-2341

[28]Jia J M, Liu S J, Cui Y, et al. *Cryst. Growth Des.*, **2013**,**13**: 4631-4634

[29]Liu S J, Zeng Y F, Xue L, et al. *Inorg. Chem. Front.*, **2014**, **1**:200-206

[30]Han S D, Miao X H, Liu S J, et al. *Chem. Asian J.*, **2014**,**9**:

3116-3120

[31]Miao X H, Han S D, Liu S J, et al. *Chin. Chem. Lett.*, **2014**, **25**:829-834

[32]Rigaku. *CrystalClear*, Process-Auto Rigaku Americas Corporation, The Woodlands, Texas, **1998**.

[33]Sheldrick G M. *SHELXL*97, *Program for Crystal Structure Refinement*, University of Göttingen, Göttingen, Germany, **1997**.

[34]Wu M F, Wang M S, Guo S P, et al. *Cryst. Growth Des.*, **2011**,**11**:372-381

[35]Kahn M L, Sutter J P, Golhen S, et al. *J. Am. Chem. Soc.*, **2000**,**122**:3413-3421

[36]Zheng Y Z, Lan Y H, Wernsdorfer W, et al. *Chem. Eur. J.*, **2009**,**15**:12566-12570

[37]Souletie J, Rabu P, Drillon M. *Phys. Rev. B*, **2005**,**72**:214427

[38]Drillon M, Panissod P, Rabu P, et al. *Phys. Rev. B*, **2002**, **65**:104404

[39]Zheng Y Z, Evangelisti M, Winpenny R E P. *Angew. Chem. Int. Ed.*, **2011**,**50**:3692-3695

[40]Zheng Y Z, Pineda E M, Helliwell M, et al. *Chem. Eur. J.*, **2012**,**18**:4161-4165

[41]FAN Shao-Yong(范少勇), HUANG Ke-Di(黄科棣), TANG Qing-Mei(唐清美), et al. *Chinese J. Inorg. Chem.*(无机化学学报), **2014**,**30**:1167-1173

[42]Peng J B, Kong X J, Zhang Q C, et al. *J. Am. Chem. Soc.*, **2014**,**136**:17938-17941

[43]Adhikary A, Jena H S, Biswas S, et al. *Chem. Asian J.*, **2014**,**9**:1083-1090

[44]Adhikary A, Sheikh J A, Biswas S, et al. *Dalton Trans.*, **2014**,**43**:9334-9343

[45]Sheikh J A, Adhikary A, Konar S. *New J. Chem.*, **2014**,**38**: 3006-3014